

# Mutual Contrastive Learning for Visual Representation Learning

Chuanguang Yang<sup>1,2</sup>, Zhulin An<sup>1\*</sup>, Linhang Cai<sup>1,2</sup>, Yongjun Xu<sup>1</sup>

<sup>1</sup>Institute of Computing Technology, Chinese Academy of Sciences, Beijing, China

<sup>2</sup>University of Chinese Academy of Sciences, Beijing, China

{yangchuanguang, anzhulin, xyj}@ict.ac.cn

## Abstract

We present a collaborative learning method called *Mutual Contrastive Learning (MCL)* for general visual representation learning. The core idea of MCL is to perform mutual interaction and transfer of contrastive distributions among a cohort of models. Benefiting from MCL, each model can learn extra contrastive knowledge from others, leading to more meaningful feature representations for visual recognition tasks. We emphasize that MCL is conceptually simple yet empirically powerful. It is a generic framework that can be applied to both supervised and self-supervised representation learning. Experimental results on supervised and self-supervised image classification, transfer learning and few-shot learning show that MCL can lead to consistent performance gains, demonstrating that MCL can guide the network to generate better feature representations.

## 1. Introduction

Contrastive learning has been widely demonstrated as an effective framework for both supervised [22, 18, 9, 30, 31, 11] and self-supervised [33, 19, 27, 16, 7, 2] visual representation learning. The core idea of contrastive learning is to pull positive pairs together and push negative pairs apart in the feature embedding space by a contrastive loss. The current pattern of contrastive learning consists of two aspects: (1) how to define positive and negative pairs; (2) how to form a contrastive loss. The main difference between supervised and self-supervised contrastive learning lies in the aspect (1). In the supervised scenario, labels often guide the definition of contrastive pairs. A positive pair is formed by two samples from the same class, while two samples from different classes form a negative pair. In the self-supervised scenario, since we do not have label information, a positive pair is often formed by two views (e.g. different data augmentations) of the same sample, while negative pairs are

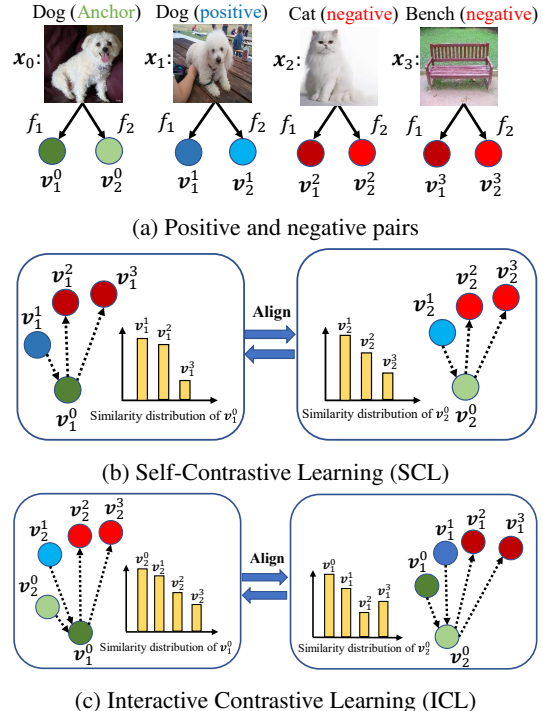


Figure 1: Overview of the proposed *Mutual Contrastive Learning*.  $f_1$  and  $f_2$  denotes two different networks.  $v_m^i$  is the embedding vector inferred from  $f_m$  with the input sample  $x_i$ . The dashed and dotted arrow denotes the direction we want to push close or apart by a contrastive loss. We also perform mutual alignment between two different softmax-based similarity distributions.

formed by different samples. Given the positive and negative pairs, we can apply a contrastive loss to generate a meaningful feature embedding space. In general, loss functions are independent of how to define pairs.

Beyond feature embedding-based learning, another vein for supervised learning aims to focus on logit-based learning. The conventional way is to train a network using cross-entropy loss between predictive class probability distribution and the one-hot ground-truth label. Some logit-based collaborative learning [38, 39, 25] methods demonstrate that a cohort of models can benefit from mutual learning of

\*Corresponding author

*class probability distributions*. Each model in such a peer-teaching manner learns better compared with learning alone in conventional supervised training. From this perspective, we hypothesize that it may be desirable to perform mutual contrastive learning among a cohort of models for learning better *feature representations*. However, existing works often train a single model to encode data points and apply contrastive learning for its own feature embedding domain. Here, all embeddings in the same domain denote that they are generated from the identical network.

By taking advantage of collaborative learning for visual representation learning, we propose a simple and generic ***Mutual Contrastive Learning*** (MCL) framework. The main core of MCL is to perform mutual interaction and transfer of contrastive distributions among a cohort of models. As illustrated in Figure 1, MCL includes Self-Contrastive Learning (SCL) and Interactive Contrastive Learning (ICL). The key distinction between SCL and ICL lies in the different contrastive embedding domains to form contrastive loss. The contrastive distribution of SCL is formed by the network’s own embedding domain, while that of ICL is formed between heterologous embedding domains derived from two different models. Furthermore, both SCL and ICL have a mimicry loss that can perform mutual alignment between different contrastive distributions from various models but formed by the same data samples. Such a peer-teaching manner with soft pseudo labels takes full advantage of representation information embedded in different models. MCL helps each model capture extra contrastive knowledge for building a more robust feature representation space.

In fact, MCL can be regarded as a group-wise contrastive loss and is orthogonal to defining positive and negative pairs. Therefore, we can readily apply MCL for both supervised and self-supervised contrastive learning. Moreover, although MCL is inspired by previous logit-based collaborative learning methods [38, 39, 25], MCL aims to capture high-order correlations in feature embedding space rather than conditionally independent class probability distribution among a cohort of models. That is to say that MCL is orthogonal to those methods and can be incorporated to train a cohort of models jointly.

We apply MCL to representation learning for a broad range of visual tasks, including supervised and self-supervised image classification, transfer learning to classification and detection, and few-shot learning. MCL can lead to consistent performance gains upon the baseline methods. Note that collaborative learning among a cohort of models is conducted during the training stage. Any network in the cohort can be kept during the inference stage. Compared with the original network, the kept network does not introduce additional inference cost.

Our main contributions are listed as follows:

- We propose a MCL framework that aims to facilitate mutual interaction and transfer of contrastive knowledge among a cohort of models.
- MCL is a new collaborative training scheme in terms of representation learning. We can naturally incorporate MCL with existing logit-based collaborative training frameworks for supervised image recognition.
- We emphasize that MCL is a simple yet powerful framework that can be applied to both supervised and self-supervised representation learning.
- Thorough experimental results show that MCL can lead to significant performance improvements across frequently-used visual tasks.

## 2. Related Work

**Contrastive Learning.** Contrastive learning has been extensively exploited for both supervised and self-supervised visual representation learning. The main idea of contrastive learning is to push positive pairs close and negative pairs apart by a contrastive loss [6]. For supervised learning, contrastive learning is often used for deep metric learning, such as face recognition [22], ReID [9] and image retrieval [18]. Triplet [32] and N-pair [24] losses upon class-aware positive and negative pairs are two widely used forms of supervised contrastive learning. Extensive improvements are also examined, for example, how to form contrastive pairs [30, 11] and samples mining [22, 31, 26].

Recently, contrastive self-supervised learning [33, 19, 27, 16, 7, 2] achieves state-of-the-art performance. The core idea is to learn invariant feature representations over human-designed pretext tasks by a contrastive loss [6, 19]. Typical pretext tasks are context auto-encoding [20] used in CPC [19], colorization [37] used in CMC [27], jigsaw [17] used in PIRL [16] and data augmentations used in SimCLR [2] and MoCo [7].

In this paper, our focus is to propose a very generic mutual contrastive learning framework. We can incorporate MCL with above advanced contrastive learning works to learn better feature representations by taking advantage of collaborative learning.

**Collaborative learning.** The idea of collaborative learning has been explored in online knowledge distillation [38, 25, 39, 1, 35, 29, 34, 13]. DML [38] shows that a group of models can benefit from mutual learning of predictive class probability distributions. CL-ILR [25] further extends this idea to a hierarchical architecture with multiple classifier heads. Recently proposed MutualNet [34] and SAN [13] conduct mutual learning among a cohort of models with various input resolutions to capture multi-scale information. All the above methods handle logit-based collaborative learning and mainly differ in the ways or inputs for knowledge transfer. Beyond logit level, Filter grafting [15] performs architecture exchange among multiple models.

Orthogonal to previous methods, we take advantage of collaborative learning from the perspective of representation learning. Moreover, we can readily incorporate MCL with previous logit-based or architecture-based methods together for collaborative learning.

### 3. Methodology

#### 3.1. Collaborative Learning Architecture

**Notation.** A classification network  $f(\cdot)$  can be divided into a feature extractor  $\varphi(\cdot)$  and a linear FC layer  $FC(\cdot)$ .  $f$  maps an input image  $x$  to a logit vector  $z$ , *i.e.*  $z = f(x) = FC(\varphi(x))$ . Moreover, we add an additional projection module  $\phi(\cdot)$  which includes two sequential FC layers with a middle ReLU.  $\phi(\cdot)$  is to transform a feature embedding from the feature extractor  $\varphi(\cdot)$  into a latent embedding  $v \in \mathbb{R}^d$ , *i.e.*  $v = \phi(\varphi(x))$ , where  $d$  is the embedding size. The embedding  $v$  is used for contrastive learning.

**Training Graph.** The overall training graph contains  $M (M \geq 2)$  classification networks denoted by  $\{f_m\}_{m=1}^M$  for collaborative learning. When  $M = 2$ , we use two independent networks  $f_1$  and  $f_2$ . When  $M > 2$ , the low-level feature layers across  $\{f_m\}_{m=1}^M$  are shared to reduce the training complexity. All the same networks in the cohort are initialized with various weights. Each  $f_m$  in the cohort is equipped with an additional embedding projection module  $\phi_m$ . The overall training graph is shown in Fig. 2a.

**Inference Graph.** During the test stage, we discard all projection modules  $\{\phi_m\}_{m=1}^M$  and keep one network for inference. The architecture of the kept network is identical to the original network. That is to say that we do not introduce extra inference cost. Moreover, we can select any  $f_m$  in the cohort for the final deployment.

#### 3.2. Mutual Contrastive Learning

##### 3.2.1 Self-Contrastive Learning

The idea of contrastive loss is to push positive pairs close and negative pairs apart in latent embedding space. Given an input sample  $x$  as the anchor, we can obtain 1 positive sample and  $K (K \geq 1)$  negative samples. For supervised learning, the positive sample is from the same class with the anchor, while negative samples are from different classes. For self-supervised learning, anchor and the positive sample are often two copies from different augmentations applied on the same instance, while negative samples are different instances. For ease of notation, we denote the anchor embedding as  $v_m^0$ , the positive embedding as  $v_m^1$  and  $K$  negative embeddings as  $\{v_m^k\}_{k=2}^{K+1}$ .  $m$  represents that the embedding is generated from  $f_m$ . Here, feature embeddings are preprocessed by  $l_2$ -normalization.

Using dot product to measure similarity distribution between anchor and contrastive embeddings with *softmax* normalization, we can obtain contrastive probability distribution

$\mathcal{P}_m = softmax([(v_m^0 \cdot v_m^1)/\tau, (v_m^0 \cdot v_m^2)/\tau, \dots, (v_m^0 \cdot v_m^{K+1})/\tau])$ , where  $\tau$  is a constant temperature.  $\mathcal{P}_m$  measures the relative sample-wise similarities with a normalized probability distribution. A large probability represents a high similarity between the anchor and a contrastive embedding. We use cross-entropy loss to force the positive pair close and negative pairs away upon the contrastive distribution  $\mathcal{P}_m$ :

$$\mathcal{L}_m^{scl\_hard} = -\log \mathcal{P}_m^0 = -\log \frac{(v_m^0 \cdot v_m^1)/\tau}{\sum_{k=1}^{K+1} (v_m^0 \cdot v_m^k)/\tau} \quad (1)$$

Here,  $\mathcal{P}_m^k$  is the  $k$ -th element of  $\mathcal{P}_m$ . This loss is equivalent to a  $(K+1)$ -way softmax-based classification loss that forces the network to classify the positive sample correctly. In fact, the form of Eq.1 is an InfoNCE loss [19], which can also be regarded as a softmax N-pair loss. The supervision is the hard one-hot label. Since contrastive distribution is learned from the network's own embedding domain, we name the Eq.1 as the hard loss of *Self-Contrastive Learning* (SCL).

Moreover, each model is also supervised by additional *soft pseudo labels* provided from other models within the cohort by **KL** divergence. For optimizing  $\mathcal{P}_m$  from  $f_m$ , the soft pseudo labels are peer contrastive distributions  $\{\mathcal{P}_l\}_{l=1, l \neq m}^{l=M}$  generated from  $\{f_l\}_{l=1, l \neq m}^{l=M}$ , respectively. The soft SCL loss of  $f_m$  is formulated as  $\mathcal{L}_m^{scl\_soft}$ .

$$\begin{aligned} \mathcal{L}_m^{scl\_soft} &= \sum_{l=1, l \neq m}^M \mathbf{KL}(\mathcal{P}_l \parallel \mathcal{P}_m) \\ &= - \sum_{l=1, l \neq m}^M \sum_{k=1}^{K+1} \mathcal{P}_l^k \log \mathcal{P}_m^k \end{aligned} \quad (2)$$

Benefiting from the soft supervisions from others, one model can gain additional teaching of contrastive knowledge. We can obtain more meaningful and robust contrastive relationships from soft calibrations. In summary, each network trained by SCL includes two supervisions from hard and soft pseudo labels. For  $M$  networks  $\{f_m\}_{m=1}^M$ , the overall SCL loss is formulated as  $\mathcal{L}_{1 \sim M}^{scl}$ .

$$\mathcal{L}_{1 \sim M}^{scl} = \sum_{m=1}^M (\mathcal{L}_m^{scl\_hard} + \mathcal{L}_m^{scl\_soft}) \quad (3)$$

##### 3.2.2 Interactive Contrastive Learning

Beyond SCL, we also perform *Interactive Contrastive Learning* (ICL) among a cohort of models. Embedding domains of various models are interactive to generate cross-view contrastive knowledge. We formulate ICL for the case of two parallel networks  $f_a$  and  $f_b$ , where  $a, b \in \{1, 2, \dots, M\}$ ,  $a \neq b$ , and then further extend ICL to more than two networks  $\{f_m\}_{m=1}^M$ .

To conduct ICL, we first fix  $f_a$  and enumerate over  $f_b$ . Given the anchor embedding  $\mathbf{v}_a^0$  extracted from  $f_a$ , we enumerate the positive embeddings  $\mathbf{v}_b^0$  as well as  $\mathbf{v}_b^1$ , and negative embeddings  $\{\mathbf{v}_b^k\}_{k=2}^{K+1}$  extracted from  $f_b$ . Here, both  $\{\mathbf{v}_a^k\}_{k=0}^{K+1}$  and  $\{\mathbf{v}_b^k\}_{k=0}^{K+1}$  are generated from the same  $K+1$  samples correspondingly, as illustrated in Fig. 1a. The contrastive probability distribution from  $f_a$  to  $f_b$  can be formulated as  $\mathcal{Q}_{a \rightarrow b} = \text{softmax}([\langle \mathbf{v}_a^0 \cdot \mathbf{v}_b^0 \rangle / \tau, \langle \mathbf{v}_a^0 \cdot \mathbf{v}_b^1 \rangle / \tau, \dots, \langle \mathbf{v}_a^0 \cdot \mathbf{v}_b^{K+1} \rangle / \tau])$ . Similar with Eq.1, we use cross-entropy loss upon the contrastive distribution  $\mathcal{Q}_{a \rightarrow b}$ :

$$\begin{aligned} \mathcal{L}_{a \rightarrow b}^{icl\_hard} &= -(\log \mathcal{Q}_{a \rightarrow b}^0 + \log \mathcal{Q}_{a \rightarrow b}^1) \\ &= -\log \frac{\langle \mathbf{v}_a^0 \cdot \mathbf{v}_b^0 \rangle / \tau + \langle \mathbf{v}_a^0 \cdot \mathbf{v}_b^1 \rangle / \tau}{\sum_{k=0}^{K+1} \langle \mathbf{v}_a^0 \cdot \mathbf{v}_b^k \rangle / \tau} \quad (4) \end{aligned}$$

Here,  $\mathcal{Q}_{a \rightarrow b}^k$  is the  $k$ -th element of  $\mathcal{Q}_{a \rightarrow b}$ . Although both  $\mathbf{v}_a^0$  and  $\mathbf{v}_b^0$  are extracted from the same sample, we also contrast  $\mathbf{v}_b^0$  as the positive embedding to  $\mathbf{v}_a^0$ . By maximizing the consensus between  $\mathbf{v}_a^0$  and  $\mathbf{v}_b^0$  from different models, we can force the network to capture more common representation information for discriminating the same sample.

We can observe that the main difference between Eq.1 and Eq.4 lies in various types of embedding domain for generating contrastive distributions. Eq.1 performs contrastive loss among feature embeddings in *self-domain* of a single network, while Eq.4 forms *cross-domain* contrastive distributions between two online networks. We term the Eq.4 as the hard loss of ICL.

Symmetrically, we can also regard  $\mathbf{v}_b^0$  extracted from  $f_b$  as the anchor, and enumerate over  $f_a$ , resulting in the contrastive probability distribution from  $f_b$  to  $f_a$  as  $\mathcal{Q}_{b \rightarrow a}$  and the interactive contrastive loss as  $\mathcal{L}_{b \rightarrow a}^{icl\_hard}$ . We further perform mutual mimicry of soft contrastive distributions between  $f_a$  and  $f_b$  by KL divergence:

$$\begin{aligned} \mathcal{L}_{a \leftrightarrow b}^{icl\_soft} &= \mathbf{KL}(\mathcal{Q}_{a \rightarrow b} \parallel \mathcal{Q}_{b \rightarrow a}) + \mathbf{KL}(\mathcal{Q}_{b \rightarrow a} \parallel \mathcal{Q}_{a \rightarrow b}) \\ &= -\sum_{k=1}^{K+1} \mathcal{Q}_{a \rightarrow b}^k \log \mathcal{Q}_{b \rightarrow a}^k - \sum_{k=1}^{K+1} \mathcal{Q}_{b \rightarrow a}^k \log \mathcal{Q}_{a \rightarrow b}^k \quad (5) \end{aligned}$$

We combine the above bidirectional interactive contrastive losses as  $\mathcal{L}_{a \leftrightarrow b}^{icl} = \mathcal{L}_{a \rightarrow b}^{icl\_hard} + \mathcal{L}_{b \rightarrow a}^{icl\_hard} + \mathcal{L}_{a \leftrightarrow b}^{icl\_soft}$ . ICL further facilitates the interaction across various embedding domains and optimizes the consistency of contrastive relationships among various models. ICL can be easily extended to more than two networks  $\{f_m\}_{m=1}^M$ . In this case, we conduct fully-connected interactive contrastive loss among  $M$  peer networks as  $\mathcal{L}_{1 \sim M}^{icl} = \sum_{1 \leq a < b \leq M} \mathcal{L}_{a \leftrightarrow b}^{icl}$ . ICL can help the cohort of models capture more informative contrastive knowledge as the number of models increases.

### 3.2.3 Overall loss of MCL

---

#### Algorithm 1 Mutual Contrastive Learning

---

```

Initialize feature extractors  $\{\varphi_m \cup \phi_m\}_{m=1}^M$ ,  $\varphi_m \in f_m$ 
while  $\{\varphi_m \cup \phi_m\}_{m=1}^M$  have not converged do
  Sample a mini-batch  $\{\mathbf{x}^{(i)}\}_{i=1}^B$ ,  $B$  is batch size
  Infer anchor embeddings  $\{\mathbf{v}_m^{0(i)}\}_{i=1}^B = \phi_m(\varphi_m(\mathbf{x}^{(i)}))_{i=1}^B$ 
  Derive contrastive embeddings  $\{\mathbf{v}_m^{k(i)}\}_{k=1}^{K+1}$  for  $\mathbf{v}_m^{0(i)}$ .
  Update  $\{\varphi_m \cup \phi_m\}_{m=1}^M$  by optimizing the Eq. 6.
end while

```

---

We summarize the losses of SCL and ICL as the overall loss for MCL among a cohort of  $M$  networks:

$$\mathcal{L}_{1 \sim M}^{MCL} = \alpha \mathcal{L}_{1 \sim M}^{scl} + \beta \mathcal{L}_{1 \sim M}^{icl} \quad (6)$$

Where  $\alpha$  and  $\beta$  are coefficients for rescaling magnitude. The overview of MCL is shown in Algorithm. 1.

### 3.3. MCL on Supervised Learning

When MCL is used for supervised learning, we create a class-aware sampler. For the mini-batch with a batch size of  $B$ , it consists of  $B/2$  classes. Each class has two samples, and others from different classes are negative samples. We derive contrastive samples from the current mini-batch.

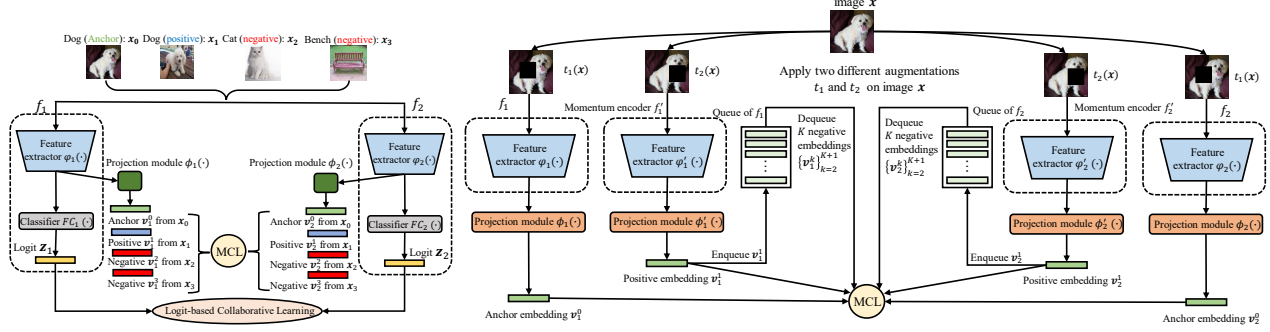
For supervised learning, we can also perform sample-independent logit-based collaborative learning from the final layer  $FC(\cdot)$ . For  $M$  networks  $\{f_m\}_{m=1}^M$  with the input  $\mathbf{x}$ , their generated logit vectors are  $\{\mathbf{z}_m\}_{m=1}^M$ , i.e.  $\mathbf{z}_m = f_m(\mathbf{x})$ . Each network is supervised by a vanilla cross-entropy loss between the predictive probability distribution and the ground-truth label. The total loss is:

$$\mathcal{L}_{1 \sim M}^{vanilla} = \sum_{m=1}^M \mathcal{L}_{ce}(\sigma(\mathbf{z}_m), y) \quad (7)$$

Where  $\sigma(\cdot)$  is softmax function,  $\mathbf{z}_m \in \mathbb{R}^C$  is the logit inferred from  $f_m$ ,  $C$  is the number of classes,  $y$  is the ground-truth label and  $\mathcal{L}_{ce}$  denotes cross-entropy loss. We further develop a simple yet powerful logit-based collaborative learning called *Ensemble Teaching* (EnsTeach) to improve the network from predictive ensemble class distributions. The loss of EnsTeach is formulated as  $\mathcal{L}^{ET}$ :

$$\mathcal{L}_{1 \sim M}^{ET} = \sum_{m=1}^M \mathbf{KL}(\sigma(\mathbf{z}_e) \parallel \sigma(\mathbf{z}_m)) \quad (8)$$

Where  $\mathbf{z}_e$  is a weighted average logit derived from  $M$  logits  $\{\mathbf{z}_m\}_{m=1}^M$ , i.e.  $\mathbf{z}_e = \sum_{m=1}^M \theta_m \mathbf{z}_m$ ,  $\theta_m \in \mathbb{R}^C$  is the weighted coefficient for  $\mathbf{z}_m$ . We regard  $\mathbf{z}_e$  as a strong *soft pseudo label* to transfer logit-level knowledge to each peer network. This is because  $\mathbf{z}_e$  adaptively fuses the predictive information from multiple networks and often performs better than any individual network. By minimizing the cross-entropy loss between  $\mathbf{z}_e$  and  $y$ , we can find out the best



(a) MCL for supervised learning

Figure 2: Overview of MCL for supervised representation learning and self-supervised representation learning.

linear coefficients  $\{\theta_m\}_{m=1}^M$ :

$$\min_{\{\theta_m\}_{m=1}^M} \mathcal{L}_{ce}(\sigma(\sum_{m=1}^M \theta_m z_m), y), \text{ s.t. } \sum_{m=1}^M \theta_m = 1, \theta_m \geq 0 \quad (9)$$

Eq.9 is a convex optimization problem and is easy to solve by linear programming. We can summarize logit-based EnTeach and embedding-based MCL as the overall loss for collaborative learning. The overall loss is  $\mathcal{L}_{1 \sim M}^{sup}$ :

$$\mathcal{L}_{1 \sim M}^{sup} = \mathcal{L}_{1 \sim M}^{vanilla} + \mathcal{L}_{1 \sim M}^{MCL} + \mathcal{L}_{1 \sim M}^{ET} \quad (10)$$

We illustrate the overview of collaborative learning under the supervised scenario as Fig. 2a.

### 3.4. MCL on Self-supervised Learning

When MCL is used for self-supervised learning, a positive pair includes two copies from different augmentations applied on the same sample, while negative pairs are often constructed from different samples. Because recent contrastive-based self-supervised learning often uses an InfoNCE loss, *i.e.* the form of Eq. 1, MCL can be readily incorporated with those great works, for example, SimCLR [2] and MoCo [7]. In this paper, we choose to combine MCL with MoCo for learning visual representation among a cohort of models. Because self-supervised learning often needs a large number of negative samples, MoCo constructs a momentum encoder and a queue for providing contrastive embeddings. Self-supervised learning only involves feature embedding-based learning so that the overall loss can be formulated as the MCL loss. We illustrate the overview of incorporating MCL with MoCo as Fig. 2b

## 4. Experiments

### 4.1. Supervised Image Classification

#### 4.1.1 Experimental Setting

**Dataset.** We use CIFAR-100 [12] and ImageNet [4] datasets. CIFAR-100 contains 50K training images and

10K test images from the label space of 100 object classes. ImageNet is a large-scale dataset including 1.2 million training images and 50K validation images from the label space of 1k classes. We adopt the standard data augmentation and preprocessing pipeline following Huang *et al.* [10].

**Hyper-parameters settings.** Following SimCLR [2], we use  $\tau = 0.1$  for CIFAR and  $\tau = 0.07$  for ImageNet in similarity calibration, and 128-d for contrastive embedding size. We use  $K = 126$  as the number of negative samples. For loss coefficients, we use  $\alpha = 0.5$  and  $\beta = 0.1$ . When the number of networks  $M > 2$ , all networks (*e.g.* ResNets [8]) share the first several convolution stages, separating from the last convolution stage on CIFAR-100 and the last two convolution stages on ImageNet. Unless otherwise specified, we use these settings for all visual tasks.

**Training settings.** For CIFAR-100, all networks are trained by SGD with a momentum of 0.9, a batch size of 128 and a weight decay of  $5 \times 10^{-4}$ . We use a cosine learning rate that starts from 0.1 and gradually decreases to 0 throughout the 300 epochs. For ImageNet, all networks are trained by SGD with a momentum of 0.9, a batch size of 256 and a weight decay of  $1 \times 10^{-4}$ . The initial learning rate starts at 0.1 and is decayed by a factor of 10 at 30, 60 and 90 epochs within the total 90 epochs. For fair comparison, we conduct all experiments with the same training settings and report the mean result over 3 runs.

#### 4.1.2 Apply MCL upon vanilla

We first investigate the efficacy of MCL upon the conventional supervised training with cross-entropy loss, as shown in Table 2. We apply widely used ResNets [8] and WRNs [36] as the backbone networks. We observe that applying MCL( $\times 2$ ) to train two networks with the same architecture jointly can lead to an average improvement of 1.77% across various architectures upon the independent training for an individual network on CIFAR-100. When extending MCL( $\times 2$ ) to MCL( $\times 4$ ) for jointly training four networks, the accuracy gains get more significant. MCL( $\times 4$ ) can result in an average improvement of 2.74% across various ar-

Model	Vanilla		DML [38]		DML [38]+MCL( $\times 2$ ) (Ours)		EnsTeach+MCL( $\times 2$ ) ( $\mathcal{L}_{1 \sim 2}^{sup}$ ) (Ours)			
	Same Arch.	Ind	Ens	Ind	Ens	Ind	Ens	Ind	Ens	Computation
ResNet-32	70.91	73.49	72.25 <sub>(+1.34)</sub>	72.59 <sub>(-0.90)</sub>	73.46 <sub>(+2.55)</sub>	73.63 <sub>(+0.14)</sub>	<b>74.56</b> <sub>(+3.65)</sub>	<b>76.14</b> <sub>(+2.65)</sub>	~ 2.12 $\times$	= 2 $\times$
ResNet-56	73.15	76.69	75.25 <sub>(+2.10)</sub>	76.72 <sub>(-0.03)</sub>	<u>76.35</u> <sub>(+3.20)</sub>	<u>77.71</u> <sub>(+1.02)</sub>	<b>76.48</b> <sub>(+3.33)</sub>	<b>78.11</b> <sub>(+1.42)</sub>	~ 2.06 $\times$	= 2 $\times$
ResNet-110	75.29	78.52	76.41 <sub>(+1.12)</sub>	77.36 <sub>(-1.16)</sub>	<u>77.81</u> <sub>(+2.52)</sub>	<u>79.47</u> <sub>(+0.95)</sub>	<b>77.92</b> <sub>(+2.63)</sub>	<b>79.58</b> <sub>(+1.06)</sub>	~ 2.04 $\times$	= 2 $\times$
WRN-16-2	72.55	74.77	73.34 <sub>(+0.79)</sub>	73.65 <sub>(-1.12)</sub>	<u>74.63</u> <sub>(+2.08)</sub>	<u>74.99</u> <sub>(+0.22)</sub>	<b>76.15</b> <sub>(+3.60)</sub>	<b>76.75</b> <sub>(+1.98)</sub>	~ 2.08 $\times$	= 2 $\times$
WRN-40-2	76.89	79.98	78.31 <sub>(+1.42)</sub>	80.16 <sub>(+0.18)</sub>	<u>79.41</u> <sub>(+2.52)</sub>	<u>80.81</u> <sub>(+0.83)</sub>	<b>79.56</b> <sub>(+2.67)</sub>	<b>80.88</b> <sub>(+0.90)</sub>	~ 2.02 $\times$	= 2 $\times$
WRN-28-4	79.17	81.13	80.05 <sub>(+0.88)</sub>	81.38 <sub>(+0.25)</sub>	<u>80.93</u> <sub>(+1.76)</sub>	<u>82.23</u> <sub>(+1.10)</sub>	<b>81.32</b> <sub>(+2.15)</sub>	<b>82.76</b> <sub>(+1.63)</sub>	~ 2.01 $\times$	= 2 $\times$
ResNet-18	69.76	71.44	70.24 <sub>(+0.48)</sub>	71.31 <sub>(-0.13)</sub>	<u>70.88</u> <sub>(+1.12)</sub>	<u>71.97</u> <sub>(+0.53)</sub>	<b>71.32</b> <sub>(+1.56)</sub>	<b>72.24</b> <sub>(+0.80)</sub>	~ 2.00 $\times$	= 2 $\times$
ResNet-34	73.30	74.85	73.86 <sub>(+0.56)</sub>	74.67 <sub>(-0.18)</sub>	<u>74.56</u> <sub>(+1.26)</sub>	<u>75.31</u> <sub>(+0.46)</sub>	<b>74.72</b> <sub>(+1.42)</sub>	<b>75.68</b> <sub>(+0.83)</sub>	~ 2.00 $\times$	= 2 $\times$

Table 1: Top-1 accuracy(%) of jointly training two networks with the same architecture on CIFAR-100 (3~8 rows) and ImageNet (last two rows). The number in brackets is the gain upon Vanilla. The **bold** number and the number in underline are row-wise best and second-best accuracy, respectively. 'Ind' and 'Ens' denote the accuracy of **Individual** network and **Ensemble**, respectively.

Model	Vanilla	+SCL(hard)	+MCL( $\times 2$ )	+MCL( $\times 4$ )
ResNet-32	70.91	71.19 <sub>(+0.28)</sub>	73.05 <sub>(+2.14)</sub>	<b>74.50</b> <sub>(+3.59)</sub>
ResNet-56	73.15	73.41 <sub>(+0.26)</sub>	74.47 <sub>(+1.32)</sub>	<b>75.92</b> <sub>(+2.77)</sub>
ResNet-110	75.29	75.72 <sub>(+0.43)</sub>	77.45 <sub>(+2.16)</sub>	<b>78.33</b> <sub>(+3.04)</sub>
WRN-16-2	72.55	72.71 <sub>(+0.16)</sub>	74.78 <sub>(+2.23)</sub>	<b>75.47</b> <sub>(+2.92)</sub>
WRN-40-2	76.89	77.01 <sub>(+0.12)</sub>	78.12 <sub>(+1.23)</sub>	<b>79.05</b> <sub>(+2.16)</sub>
WRN-28-4	79.17	79.30 <sub>(+0.13)</sub>	80.68 <sub>(+1.51)</sub>	<b>81.14</b> <sub>(+1.97)</sub>

Table 2: Top-1 accuracy (%) on CIFAR-100. Vanilla denotes training a single network with conventional cross-entropy loss ( $\mathcal{L}_1^{vanilla}$ ). SCL (hard) denotes training a single network with an extra hard contrastive loss ( $\mathcal{L}_1^{vanilla} + \mathcal{L}_1^{scl, hard}$ ).  $\times M$  denotes the number of networks in the cohort for MCL ( $\mathcal{L}_{1 \sim M}^{vanilla} + \mathcal{L}_{1 \sim M}^{MCL}$ ). The number in brackets is the gain upon vanilla.

Method	ImageNet		Pascal VOC Det mAP
	Cls Top-1	Cls Top-5	
ResNet-18+Vanilla	69.76	89.08	76.18
ResNet-18+MCL( $\times 2$ )	70.54 <sub>(+0.78)</sub>	89.97 <sub>(+0.89)</sub>	77.43 <sub>(+1.25)</sub>
ResNet-18+MCL( $\times 4$ )	71.06 <sub>(+1.30)</sub>	90.31 <sub>(+1.23)</sub>	77.88 <sub>(+1.70)</sub>
ResNet-34+Vanilla	73.30	91.42	79.31
ResNet-34+MCL( $\times 2$ )	74.35 <sub>(+1.05)</sub>	92.07 <sub>(+0.65)</sub>	80.43 <sub>(+1.12)</sub>
ResNet-34+MCL( $\times 4$ )	74.81 <sub>(+1.51)</sub>	92.43 <sub>(+1.01)</sub>	81.01 <sub>(+1.70)</sub>

Table 3: Classification accuracy (%) on ImageNet and mAP of downstream transfer learning for detection on Pascal VOC. For detection, We use Faster-RCNN [21] based on FPN [14]. The number in brackets is the gain upon vanilla.

Model	Net1	Net2	DML [38]		DML [38]+MCL (Ours)	
			Net1	Net2	Net1	Net2
ResNet-32	ResNet-56	73.49	75.45	74.97 <sub>(+1.48)</sub>	76.86 <sub>(+1.41)</sub>	
ResNet-32	WRN-16-2	73.52	75.85	74.91 <sub>(+1.39)</sub>	77.06 <sub>(+1.21)</sub>	
ResNet-32	WRN-28-4	73.42	79.86	74.98 <sub>(+1.56)</sub>	81.02 <sub>(+1.16)</sub>	
ResNet-56	ResNet-110	75.33	76.32	77.22 <sub>(+1.89)</sub>	78.44 <sub>(+2.12)</sub>	
WRN-40-2	WRN-28-4	77.96	80.35	79.40 <sub>(+1.44)</sub>	81.44 <sub>(+1.11)</sub>	
ResNet-110	WRN-28-4	76.97	80.28	77.98 <sub>(+1.01)</sub>	81.57 <sub>(+1.29)</sub>	
ResNet-18	ResNet-34	70.35	73.54	71.65 <sub>(+1.30)</sub>	74.32 <sub>(+0.78)</sub>	

Table 4: Top-1 accuracy(%) of jointly training two different networks on CIFAR-100 (3~8 rows) and ImageNet (last row). The number in brackets is the gain upon DML.

chitectures upon the vanilla on CIFAR-100. These results verify our claim that more networks in the cohort can capture more informative contrastive knowledge conducive to representation learning. Moreover, we also apply a contrastive loss to train a single network  $f_1$  for comparison, *i.e.* the hard loss of SCL as  $\mathcal{L}_1^{scl, hard}$ . We observe that the hard loss of SCL only leads to marginal improvements (*i.e.* an

average gain of 0.23%) upon baseline. Although applying a contrastive loss onto a single network somewhat improves the discriminability of feature space, MCL can guide each network to learn much more meaningful feature representations benefiting from contrastive interactions.

Extensive experiments on more challenging ImageNet further show the scalability of MCL for representation learning to the large-scale dataset. As shown in Table 3, MCL leads to consistent performance improvements on ResNet backbones in terms of top-1 and top-5 accuracy. Consistent with CIFAR-100, MCL( $\times 4$ ) often leads to a more significant gain than MCL( $\times 2$ ). For top-1 accuracy, MCL( $\times 4$ ) achieves 1.30% gain for ResNet-18 and 1.51% gain for ResNet-34 on ImageNet.

### 4.1.3 Incorporate MCL with logit-based methods

Another advantage of our feature-based MCL is that it can incorporate logit-based methods for collaborative learning. We choose DML [38], which is a widely used and effective method for logit-based mutual learning. We show all results for jointly training two networks with the same architecture in Table 1. We first examine to incorporate MCL with DML. Although DML leads to a nontrivial 1.23% improvement on average for Ind accuracy upon vanilla, incorporating DML with MCL can further bring an extra 1.21% gain on average upon DML. The result shows that MCL can be well compatible with the logit-based collaborative learning method. Moreover, we observe that Ens accuracy trained by DML often underperforms the vanilla. This is because logit-level mutual learning between two networks damages the diversity of predictive class distributions. Applying MCL onto DML can lead to better Ens accuracy with an average margin of 1.17%. This is because MCL enriches the ensemble knowledge from collaborative representation learning.

We also challenge DML with our EnsTeach. As shown in Table 1, DML+MCL achieves an average gain of 2.43% for Ind accuracy, while EnsTeach+MCL obtains an average gain of 3.01%. More importantly, EnsTeach can surpass DML with an average gain of 0.94% for Ens accuracy, in some cases by nontrivial margins, for example, on ResNet-32 and WRN-16-2. These results demonstrate that En-

Model	Vanilla		DML [38]		CL-ILR [25]		ONE [39]		OKDDip [1]		EnsTeach+MCL( $\times 4$ ) $[\mathcal{L}_{1 \sim 4}^{sup}]$ (Ours)	
Same Arch.	Ind	Ens	Ind	Ens	Ind	Ens	Ind	Ens	Ind	Ens	Ind	Ens
DenseNet-40-12	70.60	<u>73.68</u>	72.18	72.87	<u>72.11</u>	72.35	71.92	72.12	71.89	72.88	<b>74.30</b> <sub>(+2.19)</sub>	<b>76.51</b> <sub>(+2.83)</sub>
ResNet-32	70.91	<u>76.87</u>	74.66	76.84	<u>74.24</u>	75.72	74.02	75.90	74.13	76.22	<b>75.88</b> <sub>(+1.64)</sub>	<b>77.89</b> <sub>(+1.02)</sub>
ResNet-110	75.29	<u>80.56</u>	77.20	79.31	<u>78.51</u>	80.42	78.32	80.25	78.41	80.53	<b>80.35</b> <sub>(+1.84)</sub>	<b>82.06</b> <sub>(+1.10)</sub>
WRN-16-2	72.55	<u>77.28</u>	75.64	76.93	<u>74.95</u>	75.51	74.04	74.47	<u>74.99</u>	76.42	<b>77.06</b> <sub>(+2.07)</sub>	<b>79.21</b> <sub>(+1.93)</sub>
WRN-28-4	79.17	82.16	80.54	82.26	<u>80.83</u>	<u>82.32</u>	80.58	81.24	80.37	81.24	<b>82.58</b> <sub>(+1.75)</sub>	<b>83.35</b> <sub>(+1.03)</sub>
ResNet-18	69.76	<u>72.38</u>	70.45	71.66	70.59	71.53	<u>70.77</u>	72.21	70.60	72.13	<b>71.74</b> <sub>(+0.97)</sub>	<b>73.05</b> <sub>(+0.67)</sub>

Table 5: Top-1 accuracy(%) comparison of various methods for jointly training 4 networks with the same architecture on CIFAR-100 (3-7 rows) and ImageNet (last row). The number in brackets is the gain of **the best result** than the second-best.

sTeach can alleviate the homogenization problem in DML. This is because EnsTeach constructs an online weighted ensemble teacher rather than peer-to-peer mimicry in DML. We think EnsTeach is a more promising logit-based method than DML due to better Ind and Ens accuracy. Extensive experiments on ImageNet show similar observations as CIFAR-100. EnsTeach+MCL achieves the best Ind and Ens performance with nontrivial margins than vanilla and DML.

We examine the training cost introduced by MCL( $\times 2$ ). For independently training two networks with the same architecture by conventional cross-entropy loss, the training time and GPU memory are  $2\times$  than one network. For MCL, we need to compute similarity distributions with contrastive embeddings. This paper uses 128-d embedding size, 1 positive and 126 negative embeddings. Extra computation is  $4\times(1+126)\times128^2\approx8M$ . Take two ResNet-32 with total 138M computation for example, applying MCL only introduces 6% computation, *i.e.* training computation is only about  $2.12\times$  than vanilla. Since we derive contrastive embeddings in mini-batch, MCL does not introduce extra GPU memory cost.

We further incorporate MCL with DML under the different-architecture setting, as shown in Table 4. Both smaller (Net1) and larger (Net2) networks can benefit from MCL upon DML. MCL can lead to an average gain of 1.46% for Net1 and an average gain of 1.38% for Net2 on CIFAR-100. Extensive experiment on ImageNet between ResNet-18 and ResNet-34 shows that MCL produces 0.90% and 0.78% gains, respectively.

We extend two networks  $f_1$  and  $f_2$  to four networks  $f_1 \sim f_4$  for collaborative learning, and compare state-of-the-art logit-based methods DML [38], CL-ILR [25], ONE [39] and OKDDip [1]. Our EnsTeach+MCL achieves consistent performance gains for Ind and Ens accuracy over prior works. For Ind accuracy, our method surpasses the second-best results by an average margin of 1.90%. Moreover, it is hard to say which is the second-best method since different methods have their superiorities for various architectures or datasets. For Ens accuracy, we observe that previous methods often underperform the vanilla in most cases. This is because logit-level collaborative learning among multiple classifier heads damages the diversity of predictive class distributions. In contrast, our EnsTeach+MCL can consis-

Method	CIFAR-100 $\rightarrow$ STL-10		CIFAR-100 $\rightarrow$ TinyImageNet	
	Vanilla	MCL( $\times 2$ )	Vanilla	MCL( $\times 2$ )
ResNet-32	63.33	64.95 <sub>(+1.62)</sub>	28.96	30.43 <sub>(+1.47)</sub>
ResNet-56	62.89	64.79 <sub>(+1.90)</sub>	28.63	29.79 <sub>(+1.16)</sub>
ResNet-110	68.85	71.46 <sub>(+2.61)</sub>	37.43	39.78 <sub>(+2.35)</sub>
WRN-16-2	66.73	69.05 <sub>(+2.32)</sub>	32.54	33.88 <sub>(+1.34)</sub>
WRN-40-2	63.66	65.76 <sub>(+2.10)</sub>	30.31	31.59 <sub>(+1.28)</sub>
WRN-28-4	66.98	68.35 <sub>(+1.37)</sub>	32.49	34.37 <sub>(+1.88)</sub>

Table 6: Linear classification accuracy (%) of transfer learning from CIFAR-100 to STL-10 and TinyImageNet.

tently outperform vanilla with an average margin of 1.58%, especially in DenseNet [10] with 2.83% margin. Compared to other methods, MCL excavates extra contrastive knowledge beyond logit-based learning, leading to more powerful ensemble knowledge.

## 4.2. Transfer Learning

**Transferring features to classification.** The main goal of representation learning is to guide the feature extractor to produce general representations that are also linear separable for unseen datasets during training. We freeze the feature extractor trained from CIFAR-100 and train a linear classifier to execute 10-way (for STL-10 [3]) or 200-way (for TinyImageNet [4]) classification. As shown in Table 6, using MCL for training feature extractors across various architectures achieves an average gain of 1.98% on STL-10 and an average gain of 1.58% on TinyImageNet. The results indicate that MCL can improve the transferability of representations.

**Transferring features to detection.** We use pre-trained ResNet-18 on ImageNet as the backbone over Faster-RCNN [21] for downstream object detection on Pascal VOC [5]. The model is finetuned on `trainval07+12` and evaluated on `test2007` using mAP. Fine-tuning strategy is followed with the original implementation [21]. As shown in Table 3, using MCL for training feature extractors of ResNet-18 and ResNet-34 on ImageNet achieves more than 1% mAP gains consistently for downstream detection. The results demonstrate the efficacy of MCL for learning better representations for semantic recognition tasks.

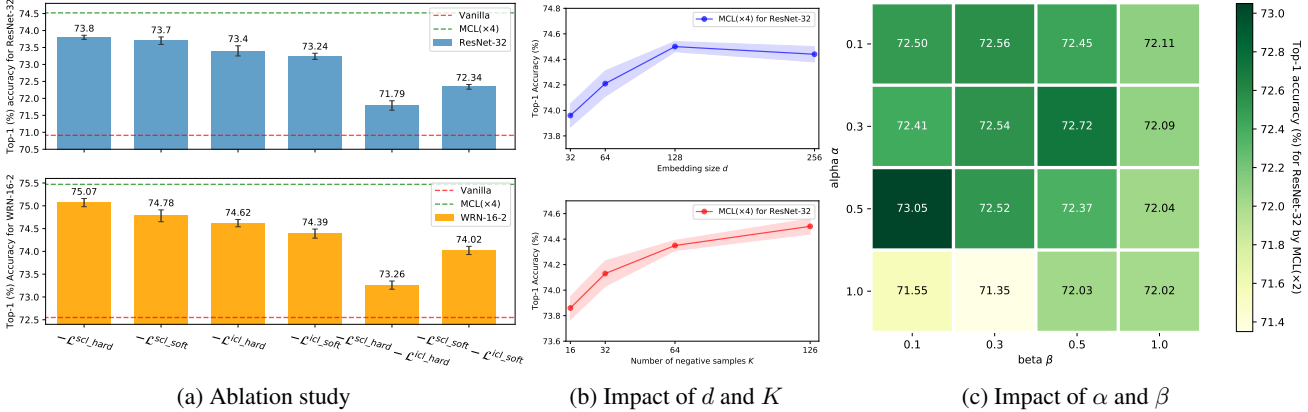


Figure 3: Ablation and hyper-parameters study on CIFAR-100.

Method	5-Way 1-Shot	5-Way 5-Shot
Prototypical network [23]	$49.10 \pm 0.82$	$66.87 \pm 0.66$
Prototypical network+MCL( $\times 2$ )	<b><math>51.63 \pm 0.78</math></b>	<b><math>68.88 \pm 0.62</math></b>

Table 7: Accuracy (%) on *miniImageNet* for few-shot learning.

Dataset	Network	#params	MoCo	MoCo+MCL( $\times 2$ )
CIFAR-100	DenseNet	0.19M	47.04	<b>48.95<sub>(+1.91)</sub></b>
	ResNet-110	1.74M	44.64	<b>46.15<sub>(+1.51)</sub></b>
	WRN-28-4	5.88M	58.34	<b>59.79<sub>(+1.45)</sub></b>
ImageNet	ResNet-50	23.77M	60.64	<b>63.21<sub>(+2.57)</sub></b>

Table 8: Top-1 Accuracy (%) on CIFAR-100 and ImageNet using MoCo [7] for self-supervised learning.

### 4.3. Few-shot Learning

We validate our proposed MCL for few-shot classification on *miniImageNet* [28] dataset. We follow the standard data pre-processing [23] and training procedure [28]. Prototypical network [23] is the backbone for generating embeddings. We apply two prototypical networks for mutually learning contrastive knowledge from each other. As the common evaluation protocol [23], we report average accuracy over 600 randomly generated episodes with 95% confidence intervals. As shown in Table 7, MCL boosts the top-1 accuracy than baseline with more than 2% margins, demonstrating that MCL can lead to a more discriminative feature embedding space.

### 4.4. MCL on Self-supervised Learning

We incorporate MCL with MoCo for self-supervised representation learning. We follow the standard experimental settings and linear classification protocol with the original MoCo [7]. In Table 8, we use two networks  $f_1$  and  $f_2$  with two peer momentum encoders  $f'_1$  and  $f'_2$  respectively, as illustrated in Fig. 2. Compared with the original MoCo, MCL leads to an average gain of 1.62% across widely used networks on CIFAR-100 and a gain of 2.57% for ResNet-50 backbone on ImageNet. The results indicate that MCL can learn better self-supervised feature representations.

### 4.5. Ablation and Hyper-parameter Study

We investigate the ablation and hyper-parameter study of MCL over supervised CIFAR-100 classification. The overall results are illustrated in Fig. 3.

**Ablation study of contrastive loss terms.** From Figure 3a, we can observe that ablating each loss term leads to performance degradation. Since accuracy reductions derived from ICL losses are more significant than that from SCL losses, we think ICL is more critical than SCL. This is because interactive contrastive knowledge from cross-domain embeddings is more informative than self-contrastive knowledge from its own embedding domain of a single model. By ablating hard losses, we found that soft losses often converge on 0 but only leads to a moderate improvement. We think that the efficacy of soft losses highly depends on the hard losses for explicitly learning diverse contrastive distributions. Moreover, ablating the soft loss also leads to a significant accuracy drop. These results suggest that both hard contrastive losses and soft mimicry losses are crucial for representation learning.

**Impact of embedding size  $d$ .** We examine the impact of embedding size  $d$  to compute contrastive distributions for MCL. We start from  $d = 32$  to  $d = 256$  and find accuracy steadily increases but saturates at  $d = 128$ .

**Impact of the number of negative samples  $K$ .** Since we mine negative samples in mini-batch and the batch size is 128, beyond one positive sample, each sample has 126 negative samples at most. We find the performance can steadily improve as  $K$  increases until the maximal 126. This observation is consistent with recent self-supervised contrastive learning [2] that more negative samples can guide the network to learn better feature representations.

**Impact of  $\alpha$  and  $\beta$ .** From Fig. 3c, we can observe that  $\alpha$  and  $\beta$  within 0.1~0.5 achieve satisfactory performance, where  $\alpha=0.5$  and  $\beta=0.1$  are the best choice.

## 5. Conclusion

We propose a simple yet effective Mutual Contrastive Learning method for collaboratively training a cohort of models from the perspective of contrastive representation learning. Experimental results show that it can enjoy a broad usage for both supervised and self-supervised learning. Moreover, we can readily incorporate MCL with existing contrastive learning works. Our method is easy to implement, and we think it may become an influential collaborative representation learning method.

## References

- [1] Defang Chen, Jian-Ping Mei, Can Wang, Yan Feng, and Chun Chen. Online knowledge distillation with diverse peers. In *AAAI*, pages 3430–3437, 2020. [2](#) [7](#)
- [2] Ting Chen, Simon Kornblith, Mohammad Norouzi, and Geoffrey Hinton. A simple framework for contrastive learning of visual representations. In *International conference on machine learning*, pages 1597–1607. PMLR, 2020. [1](#) [2](#) [5](#) [8](#)
- [3] Adam Coates, Andrew Ng, and Honglak Lee. An analysis of single-layer networks in unsupervised feature learning. In *Proceedings of the fourteenth international conference on artificial intelligence and statistics*, pages 215–223. JMLR Workshop and Conference Proceedings, 2011. [7](#)
- [4] Jia Deng, Wei Dong, Richard Socher, Li-Jia Li, Kai Li, and Li Fei-Fei. Imagenet: A large-scale hierarchical image database. In *2009 IEEE conference on computer vision and pattern recognition*, pages 248–255. Ieee, 2009. [5](#) [7](#)
- [5] Mark Everingham, Luc Van Gool, Christopher KI Williams, John Winn, and Andrew Zisserman. The pascal visual object classes (voc) challenge. *International journal of computer vision*, 88(2):303–338, 2010. [7](#)
- [6] Raia Hadsell, Sumit Chopra, and Yann LeCun. Dimensionality reduction by learning an invariant mapping. In *2006 IEEE Computer Society Conference on Computer Vision and Pattern Recognition (CVPR’06)*, volume 2, pages 1735–1742. IEEE, 2006. [2](#)
- [7] Kaiming He, Haoqi Fan, Yuxin Wu, Saining Xie, and Ross Girshick. Momentum contrast for unsupervised visual representation learning. In *Proceedings of the IEEE/CVF Conference on Computer Vision and Pattern Recognition*, pages 9729–9738, 2020. [1](#) [2](#) [5](#) [8](#)
- [8] Kaiming He, Xiangyu Zhang, Shaoqing Ren, and Jian Sun. Deep residual learning for image recognition. In *Proceedings of the IEEE conference on computer vision and pattern recognition*, pages 770–778, 2016. [5](#)
- [9] Alexander Hermans, Lucas Beyer, and Bastian Leibe. In defense of the triplet loss for person re-identification. *arXiv preprint arXiv:1703.07737*, 2017. [1](#) [2](#)
- [10] Gao Huang, Zhuang Liu, Laurens Van Der Maaten, and Kilian Q Weinberger. Densely connected convolutional networks. In *Proceedings of the IEEE conference on computer vision and pattern recognition*, pages 4700–4708, 2017. [5](#) [7](#)
- [11] Prannay Khosla, Piotr Teterwak, Chen Wang, Aaron Sarna, Yonglong Tian, Phillip Isola, Aaron Maschinot, Ce Liu, and Dilip Krishnan. Supervised contrastive learning. *arXiv preprint arXiv:2004.11362*, 2020. [1](#) [2](#)
- [12] Alex Krizhevsky, Geoffrey Hinton, et al. Learning multiple layers of features from tiny images. 2009. [5](#)
- [13] Duo Li, Anbang Yao, and Qifeng Chen. Learning to learn parameterized classification networks for scalable input images. In *European Conference on Computer Vision*, pages 19–35. Springer, 2020. [2](#)
- [14] Tsung-Yi Lin, Piotr Dollár, Ross Girshick, Kaiming He, Bharath Hariharan, and Serge Belongie. Feature pyramid networks for object detection. In *Proceedings of the IEEE conference on computer vision and pattern recognition*, pages 2117–2125, 2017. [6](#)
- [15] Fanxu Meng, Hao Cheng, Ke Li, Zhixin Xu, Rongrong Ji, Xing Sun, and Guangming Lu. Filter grafting for deep neural networks. In *Proceedings of the IEEE/CVF Conference on Computer Vision and Pattern Recognition*, pages 6599–6607, 2020. [2](#)
- [16] Ishan Misra and Laurens van der Maaten. Self-supervised learning of pretext-invariant representations. In *Proceedings of the IEEE/CVF Conference on Computer Vision and Pattern Recognition*, pages 6707–6717, 2020. [1](#) [2](#)
- [17] Mehdi Noroozi and Paolo Favaro. Unsupervised learning of visual representations by solving jigsaw puzzles. In *European Conference on Computer Vision*, pages 69–84. Springer, 2016. [2](#)
- [18] Hyun Oh Song, Yu Xiang, Stefanie Jegelka, and Silvio Savarese. Deep metric learning via lifted structured feature embedding. In *Proceedings of the IEEE conference on computer vision and pattern recognition*, pages 4004–4012, 2016. [1](#) [2](#)
- [19] Aaron van den Oord, Yazhe Li, and Oriol Vinyals. Representation learning with contrastive predictive coding. *arXiv preprint arXiv:1807.03748*, 2018. [1](#) [2](#) [3](#)
- [20] Deepak Pathak, Philipp Krahenbuhl, Jeff Donahue, Trevor Darrell, and Alexei A Efros. Context encoders: Feature learning by inpainting. In *Proceedings of the IEEE conference on computer vision and pattern recognition*, pages 2536–2544, 2016. [2](#)
- [21] Shaoqing Ren, Kaiming He, Ross Girshick, and Jian Sun. Faster r-cnn: Towards real-time object detection with region proposal networks. *IEEE transactions on pattern analysis and machine intelligence*, 39(6):1137–1149, 2016. [6](#) [7](#)
- [22] Florian Schroff, Dmitry Kalenichenko, and James Philbin. Facenet: A unified embedding for face recognition and clustering. In *Proceedings of the IEEE conference on computer vision and pattern recognition*, pages 815–823, 2015. [1](#) [2](#)
- [23] Jake Snell, Kevin Swersky, and Richard Zemel. Prototypical networks for few-shot learning. In *Advances in neural information processing systems*, pages 4077–4087, 2017. [8](#)
- [24] Kihyuk Sohn. Improved deep metric learning with multi-class n-pair loss objective. In *Advances in neural information processing systems*, pages 1857–1865, 2016. [2](#)
- [25] Guocong Song and Wei Chai. Collaborative learning for deep neural networks. In *Advances in Neural Information Processing Systems*, pages 1832–1841, 2018. [1](#) [2](#) [7](#)

- [26] Yumin Suh, Bohyung Han, Wonsik Kim, and Kyoung Mu Lee. Stochastic class-based hard example mining for deep metric learning. In *Proceedings of the IEEE/CVF Conference on Computer Vision and Pattern Recognition*, pages 7251–7259, 2019. [2](#)
- [27] Yonglong Tian, Dilip Krishnan, and Phillip Isola. Contrastive multiview coding. *arXiv preprint arXiv:1906.05849*, 2019. [1](#), [2](#)
- [28] Oriol Vinyals, Charles Blundell, Timothy Lillicrap, Daan Wierstra, et al. Matching networks for one shot learning. In *Advances in neural information processing systems*, pages 3630–3638, 2016. [8](#)
- [29] Devesh Walawalkar, Zhiqiang Shen, and Marios Savvides. Online ensemble model compression using knowledge distillation. In *European Conference on Computer Vision*, pages 18–35. Springer, 2020. [2](#)
- [30] Xinshao Wang, Yang Hua, Elyor Kodirov, Guosheng Hu, Romain Garnier, and Neil M Robertson. Ranked list loss for deep metric learning. In *Proceedings of the IEEE/CVF Conference on Computer Vision and Pattern Recognition*, pages 5207–5216, 2019. [1](#), [2](#)
- [31] Xinshao Wang, Yang Hua, Elyor Kodirov, Guosheng Hu, and Neil M Robertson. Deep metric learning by online soft mining and class-aware attention. In *Proceedings of the AAAI Conference on Artificial Intelligence*, volume 33, pages 5361–5368, 2019. [1](#), [2](#)
- [32] Kilian Q Weinberger and Lawrence K Saul. Distance metric learning for large margin nearest neighbor classification. *Journal of Machine Learning Research*, 10(2), 2009. [2](#)
- [33] Zhirong Wu, Yuanjun Xiong, Stella X Yu, and Dahua Lin. Unsupervised feature learning via non-parametric instance discrimination. In *Proceedings of the IEEE Conference on Computer Vision and Pattern Recognition*, pages 3733–3742, 2018. [1](#), [2](#)
- [34] Taojiannan Yang, Sijie Zhu, Chen Chen, Shen Yan, Mi Zhang, and Andrew Willis. Mutualnet: Adaptive convnet via mutual learning from network width and resolution. In *European Conference on Computer Vision (ECCV)*, 2020. [2](#)
- [35] Anbang Yao and Dawei Sun. Knowledge transfer via dense cross-layer mutual-distillation. In *European Conference on Computer Vision*, pages 294–311. Springer, 2020. [2](#)
- [36] Komodakis N Zagoruyko S. Wide residual networks. In *Proceedings of the British Machine Vision Conference*, 2016. [5](#)
- [37] Richard Zhang, Phillip Isola, and Alexei A Efros. Colorful image colorization. In *European conference on computer vision*, pages 649–666. Springer, 2016. [2](#)
- [38] Ying Zhang, Tao Xiang, Timothy M Hospedales, and Huchuan Lu. Deep mutual learning. In *Proceedings of the IEEE Conference on Computer Vision and Pattern Recognition*, pages 4320–4328, 2018. [1](#), [2](#), [6](#), [7](#)
- [39] Xiatian Zhu, Shaogang Gong, et al. Knowledge distillation by on-the-fly native ensemble. In *Advances in neural information processing systems*, pages 7517–7527, 2018. [1](#), [2](#), [7](#)